Proceedings of 9th International Symposium on Fluid-Structure Interactions, Flow-Sound Interactions, Flow-Induced Vibration & Noise
July 8-11, 2018, Toronto, Ontario, Canada

FIV2018-163

CFD ESTIMATION OF DAMPING-CONTROLLED FLUIDELASTIC INSTABILITY MAPS DEPENDENCE ON ARRAY PITCH RATIO

Beatriz de Pedro
School of Engineering
University of Oviedo
Spain
pedrobeatriz@uniovi.es

Craig Meskell
School of Engineering
Trinity College Dublin
Ireland
cmeskell@tcd.ie

ABSTRACT

Tube arrays subject to cross flow may exhibit large amplitude self excited vibrations referred to as Fluidelastic Instability (FEI). Experimental data as well as other studies indicate that the stability threshold is strongly dependent on the pitch-ratio of the array. In damping-controlled FEI, although only a single structural degree of freedom is needed, the fluid dynamics are inherently unsteady. Instability occurs when the total net damping (structural plus fluid) reduces to zero. Here, a series of simulations using a dynamic-mesh URANS solver for increasing velocities below the stability threshold are carried out in free motion conditions. The free decay of tube response in the stable regime allows the net damping to be calculated and hence the damping-velocity curves can be obtained yielding the zero net damping point. Since RANS does not simulate turbulent buffeting, the flow-structure system reponse is effectively deterministic. This allows very small amplitudes to be investigated which is advantageous for two reasons. Firstly, small amplitudes facilitate the moving mesh approach. Secondly, as the amplitudes are small, the non-linear fluid damping and stiffness components are negligible as these are cubic in form. These non-linearities lead to to limit cycle oscillations in a post stable regime and more importantly bias linear damping estimates in the stable regime. The procedure has been repeated to yield estimates of damping for a range of mass-damping (20-100) in seven normal triangular with pitch ratios ranging from 1.25 to 1.58. The FEI threshold for pitch ratio of 1.58 was found to be approximately twice that for a pitch ratio of 1.25. The ultimate aim is to propose an algebraic expression to account for the variation due to pitch ratio. This has not been achieved as the dataset is still to small, but the characteristics of the algebraic function have been determined.

NOMENCLATURE

m	Tube mass
L	Tube length
m_r	Mass ratio
P	Pitch length
U_c	Critical reduced gap velocity
U_r	Reduced gap velocity
U_0	Upstream velocity
δ	Structural damping
δ_{net}	Coupled system net damping
ρ	Fluid density

INTRODUCTION

Flow-induced vibration (FIV) can be a major problem in large heat exchangers leading to shut down or even decommissioning. While turbulent buffeting and the associated wear represents a limit on the long term integrity of these assemblies, fluidelastic instability (FEI) can lead to failure in the short term. As a result, FEI represents a limitation on the operational parameters of the unit. One particular mechanism of FEI, so-called damping controlled instability, can occur when a single flexible tube is subjected to cross flow, even within an otherwise rigid array. It is this mechanism which is the focus of the current study. A comprehensive introduction to FEI in tube arrays can be found in, for example, Chapter 5 of Paidoussis et al. [1] and a review of available models for specifically for damping controlled fluidelastic instability is given by Price [2].

Previous models of FEI and schemes for collapsing experimental data sets of critical velocity have assumed that the Reynolds number, mass ratio or pitch ratio have no effect on levels of critical velocity. However, there is some experimental and analytical studies indicating that this may not be the case (e.g. [3], [4], [5], [6]).

In a previous study, de Pedro and Meskell [7] evaluated the specific dependence of critical velocity on those three factors (mass ratio, Reynolds number and pitch ratio) by means of an hybrid analytical-CFD methodology. One of the key conclusions of this study was that the pitch ratio had the most significant effect on the instability onset. The objective of the present study is to determinate critical velocity dependence on pitch ratio and reduce it to a single algebraic expression for noraml triangular arrays.

CFD METHODOLOGY

In the present work the methodology will be purely numerical, consisting in series of dynamic-mesh Unsteady Reynolds Averaged Navier-Stokes (URANS) calculations capturing the tube amplitude of free decay vibration in stable conditions. The critical velocity can be then predicted by extrapolating damping trend decrease to zero. Small amplitudes were considered in order to facilitate dynamic mesh calculations. In addition, as the fluidelastic force is non-linear in the the vibration amplitude with cubic form [8], a small amplitude vibration allows the higher order (non-linear) components to be ignored. At these low amplitudes, the non-linear fluid damping and stiffness components that can lead to limit cycle oscillations in a post stable regime are negligible. Simulated the flow field using URANS does generate turbulent buffeting excitation and so the coupled flow-structure system is effectively deterministic. Thus, it is possible to obtain the underlying free decay behaviour even at very low amplitudes are possible without the need for ensemble averaging to remove the turbulent buffeting. By using an unsteady simulation, with the tube motion determined by the fluid force rather than prescribed, it is hoped that the important physical mechanisms responsible for damping controlled FEI are simulated, without the need for a semi-empirical model.

In order to assess the sensitivity of the critical velocity to pitch ratio, the unsteady flow through a normal triangular tube array was modeled using ANSYS-Fluent 17 for seven different arrays, with pitch-to-diameter ratios in the range 1.25 to 1.58. In all cases, the array consisted of five rows of cylinders, each with either six whole cylinders or five whole cylinders plus two halves attached to each side. The cylinder diameter was always 38 mm. Figure 1 shows the schematic of the typical domain used. The numerical domain extended both upstream and downstream from the cylinder array nine tube diameters.

Several preliminary computations were performed in order to select adequate calculation parameters including turbulence model (k-ε RNG, non-equilibrium wall functions), boundary conditions at the channel sides (periodic), mesh refinement and time step. The ultimate choice of turbulence model should be noted. The family of k-ε models are known to perform badly in terms of estimating drag forces. However, by comparing the simulated surface pressure distribution with experimental data from the literature, it was found that the k-ε RNG was superior than, for example, the SST model. This is an important point, as the choice of turbulence model may be the cause of significant overestimation of the stability threshold, as will be discussed below. Another key feature of the numerical approach adopted is the inclusion of full-slip guide plates behind each tube of the last row, parallel to the main stream. These plates prevent the appearance of large-scale flow oscillations downstream which may be responsible for bistable flow reported in the literature.

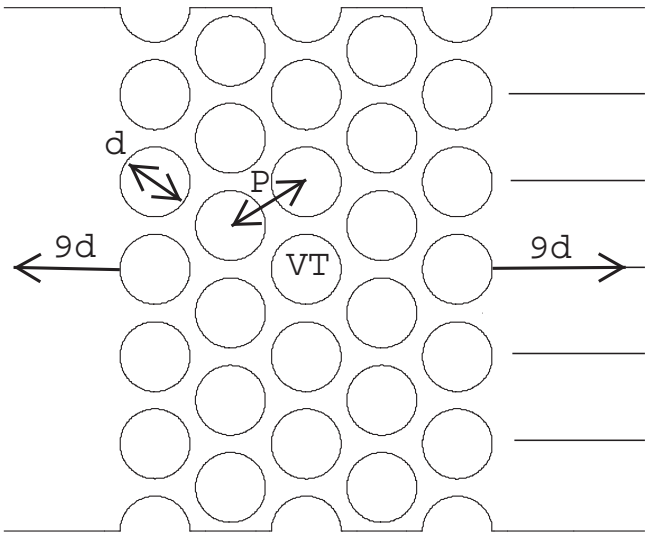

FIGURE 1: SCHEMATIC OF THE COMPUTATIONAL DOMAIN.

This was preferred to the approach of truncating the domain at the centerline of the last cylinder row as used in other studies (e.g. [10]). The use of the guide plates allows the outlet pressure boundary condition to be placed sufficiently far downstream that it can be assumed that it does not interfere directly with the flow inside the array. Further details from these preliminary simulations can be found in a previous study [9].

To discretize the domain, a refined grid (Fig. 2) was used around each cylinder in the array that was composed of quadrilateral cells with an initial thickness of 0.06 mm at the tube wall and a growth factor of 1.15 in the radial direction until the 13th line. This ensured y^+ values of the order of approximately 1 for all the simulations conducted. The rest of the domain was meshed with triangular elements of progressively greater size upstream and downstream of the array.

To incorporate the motion of the vibrating tube, the CFD model was complemented with an additional subroutine (User Defined Function) controlling the tube motion so that, at every time step, the position of the tube is updated and the domain remeshed (see [9] for details).

This numerical procedure is based on previous studies [9], [7] and [11]. In the development of this approach, the performance of the scheme has been compared to several datasets in the literature: tube

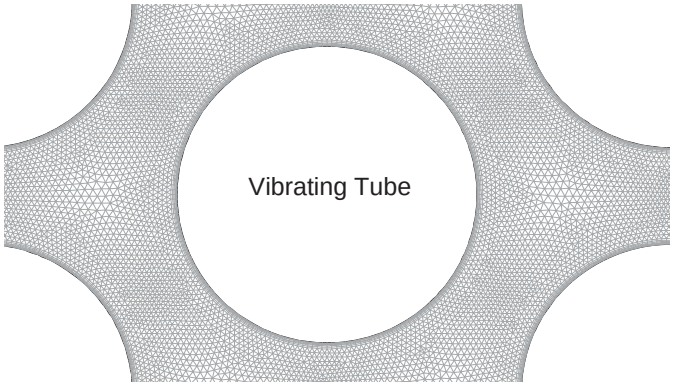

FIGURE 2: DETAIL OF THE MESH IN THE INTER-CYLINDER REGION.

surface pressure distribution measurements obtained by Mahon and Meskell [12]; critical velocity prediction for the two normal triangular arrays tested by Austermann and Popp [13]; time delay between lift coefficient and tube motion measured by Mahon and Meskell [14]; velocity fluctuations along fluid lines amplitude and phase obtained by Khalifa et al. [15]; lift coefficient amplitude and phase curves evolution with reduced gap velocity measured by Sawadogo and Mureithi [16]. These comparisons of the methodology with previously published data offer some confidence in the reliability of the approach to capture the variation of FEI phenomenon with pitch ratio.

In this study, critical velocity predictions are obtained from extrapolating the trend of the apparent net damping of the coupled system close to the critical velocity in stable conditions. In order to obtain this trend, the net damping is estimated for a number of stable reduced flow velocities. At each flow velocity, the tube is set free from an initial displacement of $0.02 \cdot d$ in the transverse direction (i.e. normal to bulk flow direction) measured from its geometrical neutral position. The system net damping can be estimated from tube free decay of the tube at each cross-flow velocity value by assuming an exponential decay associated with a linear single degree of freedom system. This assumption is justified by the small vibration amplitudes; the non-linear fluid damping and stiffness components that can lead to limit cycle oscillations in a post stable regime are negligible as these are cubic. In order to eliminate the possibility of numerical transients (due to the initialization of the sim-

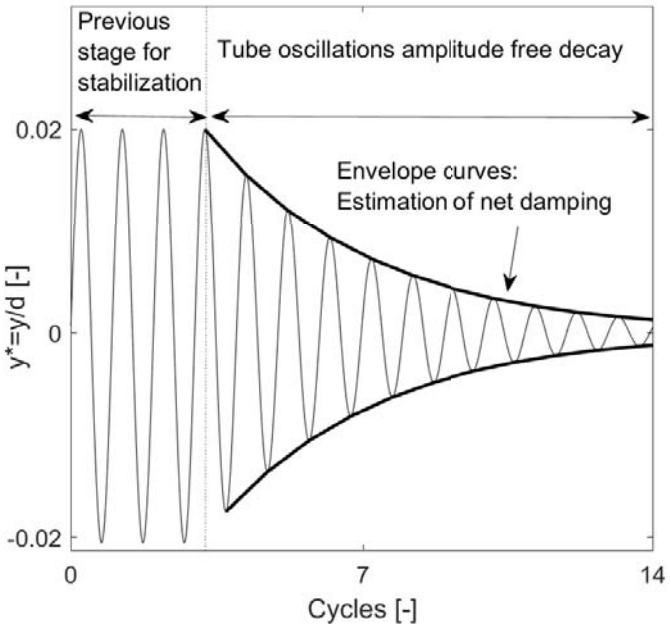

FIGURE 3: CFD PREDICTION OF REDUCED CRITICAL VELOCITY U_c.

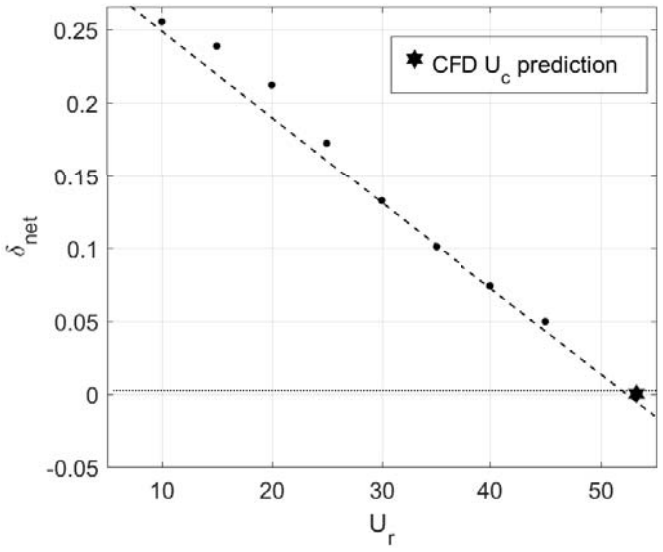

FIGURE 4: CFD PREDICTION OF REDUCED CRITICAL VELOCITY U_c.

ulation), the tube is initially forced sinusoidally to yield an amplitude of $0.02 \cdot d$ and then released at maximum displacement. Figure 3 shows a typical time trace of the simulated tube motion. The cross flow velocity is chosen to be below the stability threshold and so the tube response is always dynamically stable, yielding positive total damping values. The steady-forced/free-decay simulation procedure is repeated for each flow velocity, mass-damping value and pitch ratio.

When cross-flow velocity approaches U_c net damping decreases. The trend obtained is extrapolated with a linear trend to the $\delta_{net} = 0$ point. This intercept is the critical velocity. Figure 4 illustrates the process of prediction of the critical velocity. The assumption that the trend of the net damping is linear in the flow velocity is supported both by direct experimental data (e.g. [8]) and by theoretical models (e.g. quasi-steady theory).

It is important to note that present work is focused on the investigation of the stability threshold dependence on pitch ratio rather than in determining the critical velocity *per se*. However, in order to provide an idea of the accuracy, this method for delimiting the critical velocity was applied to the three mass damping parameter simulated in this investigation and compared to equivalent stability threshold values measured by Austermann and Popp [13] for the same geometry. Figure 5 shows comparison results with this particular methodology and the data are tabulated Table 1. As can be seen in both figure and table the CFD stability threshold is systematically overestimated by roughly a 25% of the experimental value. The cause of this systematic over-prediction is not clear. There are two possibilities. The first possible cause is that a A URANS model is effectively deterministic, the effect of random turbulent buffeting is simply not present. This is an advantage for data processing to obtain the damping, but excludes that possibility that turbulent buffeting and fluidelastic instability interact. Rzentkowski and Lever [17] suggested that the onset of instability could be reduced by upto 20% by the presence of turbulence, albeit in a square array. This was based on a non-linear theoretical model, with very limited experimental evidence. Here we have argued that the low amplitudes inherently render the nonlinear natural of the fluidelastic force negligible, so it would be incompatible to rely on this to explain the discrepancy. Furthermore, it seems unlikely that the simulation is underestimating the negative damping effects by such a large degree as these are determined by convection processes yielding a phase between tube motion and fluid force. This phase difference had been previously assessed and compared with experimental data and found to be in good agreement [9].

$m_r\delta$	$U_{c,exp}$	$U_{c,CFD}$	$\varepsilon_r = (\frac{U_{c,CFD}}{U_{c,exp}} - 1) * 100$
20	15.987	19.97	24.9%
50	26.077	32.82	25.6%
100	42.891	53.23	24.1%

TABLE 1: CFD U_c PREDICTIONS RELATIVE DIFFERENCE TO EXPERIMENTAL THRESHOLD FOR THE $P/d = 1.25$ array. $m_r\delta$=20, 50 and 100.

This would imply that the second possible explanation of the discrepancy in the critical velocity is more likely, namely that the simulation is overestimating the positive fluid damping. The separation region in the immediate wake of the tube will probably be underestimated as a k-ε has been used. Therefore, the simulation is either overestimating the skin friction, which is likely with a wall function, and/or the degree to which the apparent fluid force is rotated by the quasi-steady effect of the tube motion is being overestimated. It should be noted that the conditions for the quasi-steady assumption are not met in a tube array, precisely because of the relative motion of the tubes, but it is a useful device to understand what may be occurring. The quasi-steady assumption causes the fluid force system (i.e. instantaneous lift and drag) to rotate so as to be aligned with the instantaneous apparent flow direction, which is the vectoral sum of the mean flow and the instantaneous tube motion. The quasi-steady assumption fails because of the proximity of other tubes and their wakes which are stationary. The use of the k-ε model underestimates the size of the near wake behind all the tubes (not just the moving tube), and so the flow field is less constrained. As a result, a greater proportion of the lift force is made to act in the transverse direction, increasing the apparent positive fluid damping. While these explanations are speculative, the overestimation of critical velocity was found to be consistent for the three mass damping parameters mapped in the present analysis. As the study envisioned here is comparative, focused on the trend rather than on the absolute accuracy of the predictions, it is concluded that the approach may be sufficient to conduct the parameter dependency analysis proposed, but some caution is advised.

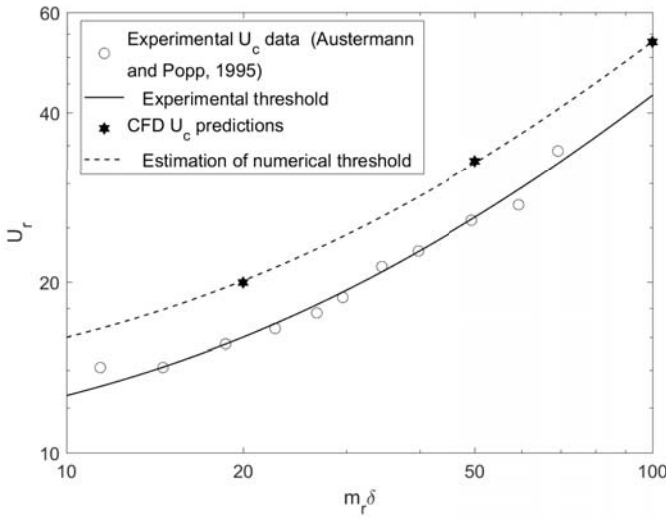

FIGURE 5: COMPARISON OF CFD THRESHOLD ESTIMATION TO EXPERIMENTAL DATA FOR $P/d = 1.25$ ARRAY.

RESULTS AND DISCUSSION

Using the numerical model described above, the effect of pitch ratio P/d in the reduced critical velocity for different mass-damping parameters has been estimated with the aim of obtaining a stability threshold surface in the three dimensional parameter space ($m_r\delta$, U_c, P/d). Results after 168 series of steady-forced/free-decay simulations are presented in this work. Those results corresponds to three values of mass damping $m_r\delta$ and seven pitch ratios P/d values. For each condition, the critical velocity was obtained with a linear fit of eight net positive damping values at subcritical flow velocities.

For $m_r\delta$=20 and $m_r\delta$=100, seven pitch ratios were considered (P/d= 1.25, 1.30, 1.32, 1.35, 1.44, 1.52 and 1.58). For $m_r\delta$=50 simulations for P/d=1.32 were not completed. For each array and each mass damping parameter, 8 subcritical flow velocities were simulated and the net damping values extracted. The reduced velocity ranges were $U_r = 5$ to 12 for $m_r\delta$=20; $U_r = 16$ to 30 for $m_r\delta$=50; and $U_r = 10$ to 45 for $m_r\delta$=100. The net damping obtained for each simulation is shown in Figure 6 for $m_r\delta$=20; Figure 7 for $m_r\delta$=50; and Figure 8 for $m_r\delta$=100. For all pitch ratios, the net damping follows a linear trend with flow velocity as expected. The critical velocity can therefore be extracted and these are projected onto the zero damping plane in Figures 6-8. The critical

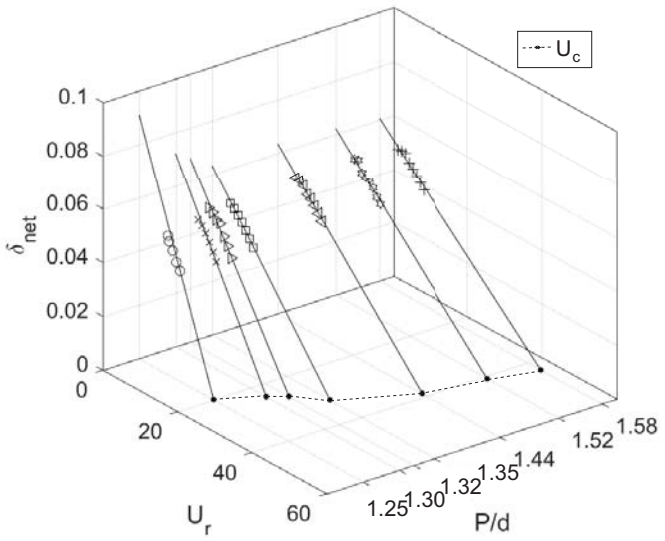

FIGURE 6: Variation of net damping for $m_r\delta$=20.

P/d	a	b	U_r	$U_r/U_{r1.25}$
1.25	0.09092	−0.00455	19.97	1.00
1.30	0.07214	−0.00297	24.31	1.22
1.32	0.06860	−0.00259	26.50	1.33
1.35	0.06330	−0.00200	31.63	1.58
1.44	0.06367	−0.00164	38.82	1.94
1.52	0.06209	−0.00151	41.04	2.06
1.58	0.06075	−0.00139	43.62	2.18

TABLE 2: Comparison of critical velocities predicted for $\delta = a + b \cdot U_r$ and $\delta = 0$ with increasing P/d arrays at $m_r\delta$=20.

velocity data and the fitted linear trend of the net damping for each pitch ratio are shown in Table 2 for $m_r\delta$=20; Table 3 for $m_r\delta$=50; Table 4 for $m_r\delta$=100. In all three mass tables the critical velocity has been normalized by the value for $P/d = 1.25$. As can be seen this factor increases montonically upto approximately 2 as pitch ratio increases.

Figure 9 shows the variation of the critical velocity with pitch ratio for the three mass-damping values modeled. The three datasets follow a similar trend, however it is not clear whether the deviation from a linear trend is

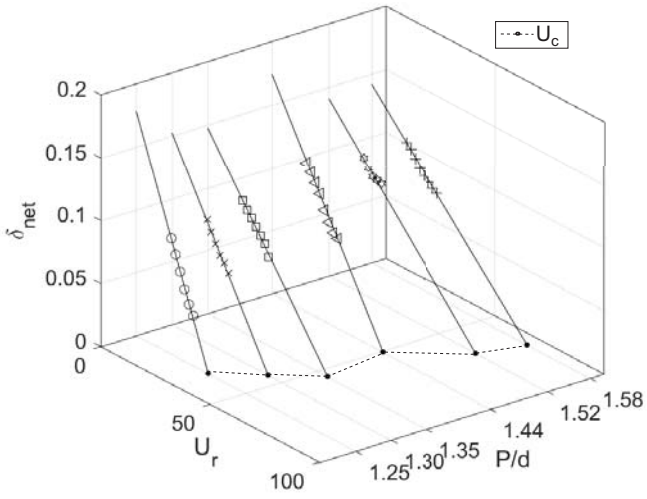

FIGURE 7: Variation of net damping for $m_r\delta$=50.

P/d	a	b	U_r	$U_r/U_{r1.25}$
1.25	0.1782	−0.005430	32.82	1.00
1.30	0.1524	−0.003475	43.86	1.34
1.35	0.1476	−0.002695	54.78	1.67
1.44	0.1743	−0.003433	50.77	1.55
1.52	0.1407	−0.002085	67.48	2.06
1.58	0.1415	−0.001980	71.47	2.18

TABLE 3: Comparison of critical velocities predicted for $\delta = a + b \cdot U_r$ and $\delta = 0$ with increasing P/d arrays at $m_r\delta$=50.

due to estimation error in the prediction procedure or is indicative of real variation. If a linear trend was assumed for each mass-damping , the maximum deviation from a linear trend would be approximately 10% - i.e. comparable to the level of uncertainty introduced by the systematic overestimation of discussed above. On the other hand, if the data is regarded as being exact, a low order polynomial surface would be sufficient to interpolate the space. Such a surface fit is shown in Fig. 10. However, at this stage, it is simply not possible to resolve which is the most appropriate approach to the overall goal of a single algrebaic expression to predict critical velocity as the data is too sparse.

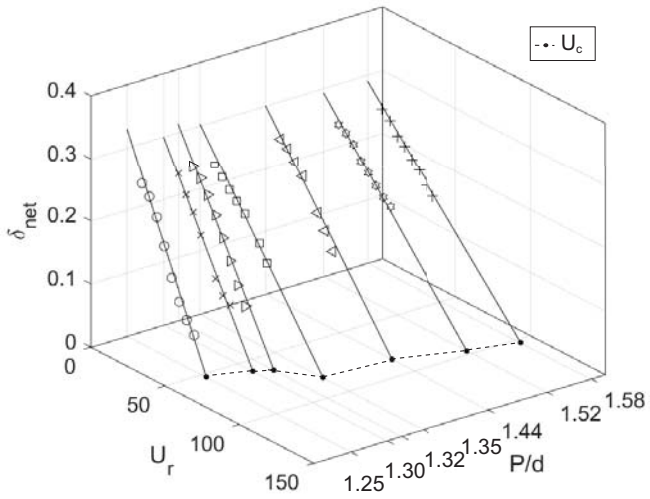

FIGURE 8: Variation of net damping for $m_r\delta$=100.

P/d	a	b	U_r	$U_r/U_{r1.25}$
1.25	0.3300	−0.006200	53.23	1.00
1.30	0.3000	−0.005000	60.00	1.13
1.32	0.3137	−0.004878	64.31	1.21
1.35	0.3036	−0.003661	82.65	1.55
1.44	0.3002	−0.003534	84.95	1.59
1.52	0.2918	−0.003005	97.10	1.82
1.58	0.2900	−0.002800	103.60	1.95

TABLE 4: Comparison of critical velocities predicted for $\delta = a + b \cdot U_r$ and $\delta = 0$ with increasing P/d arrays at $m_r\delta$=100.

CONCLUSION

A CFD methodology for the critical velocity prediction has been proposed using dynamic-mesh URANS simulations. Two specific conclusions were found at this point of the investigation:

1. the unsteady simulation of the fully coupled flow-structure system tends to overestimate the critical velocity by approximately 25%. This has been attributed to the choice of turbulence model in the URANS calculations.
2. the effect of increasing the pitch ratio from $P/d = 1.25$ to $P/d = 1.58$ is to approximately double the reduced velocity, and this is consistent for mass ratio $m_r\delta$=20,50 and 100.

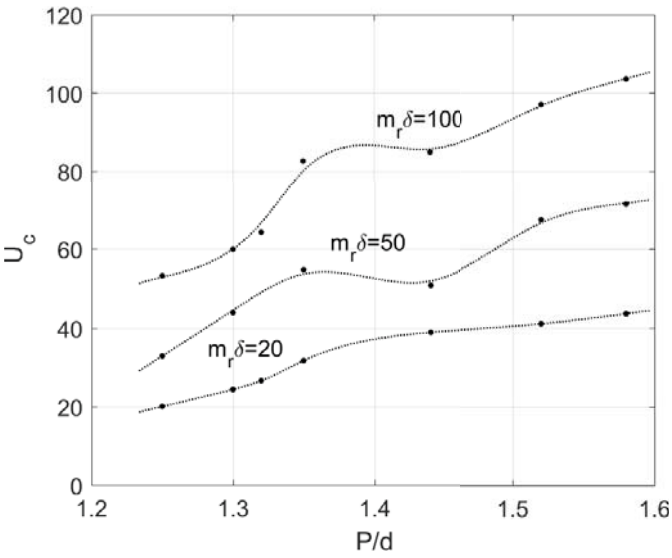

FIGURE 9: CRITICAL VELOCITY DEPENDENCE ON PITCH RATIO AT DIFFERENT STABILITY MAP ABSCESSES POSITIONS.

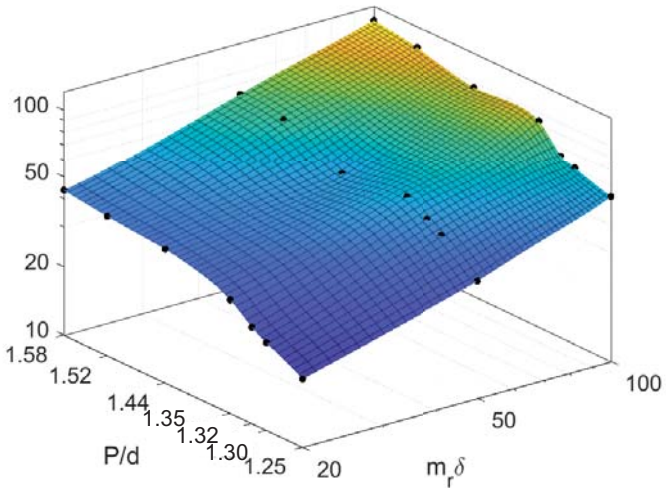

FIGURE 10: CRITICAL VELOCITY SURFACE AS A FUNCTION OF $m_r\delta$ AND P/d.

While the ultimate goal of a simple expression for the variation of critical velocity with pitch ratio could not yet be achieved with confidence, nonetheless, the overall methodology is encouraging.

ACKNOWLEDGMENT

The authors gratefully acknowledge the financial support of the Principality of Asturias Government under the PhD grant BP-12054 awarded to Ms. de Pedro and the financial support of Science Foundation Ireland under the SFI Strategic Partnership Programme Grant Number SFI/15/SPP/E3125.

REFERENCES

[1] Païdoussis, M. P., Price, S., de Langre, E., 2011. "Fluid-Structure Interactions Cross flow instabilities.". *Cambridge University Press, Cambridge*

[2] Price, S. J.,1995. "A Review of Theoretical Models for Fluidelastic Instability of Cylinder Arrays in Cross-Flow". *Journal of Fluids and Structures,* ***9***, pp. 463–518.

[3] Mewes, D. and Stockmeier, D., 1991. "A new model for damping controlled fluidelastic instability in heat exchanger tube arrays". *In Flow Induced Vibrations*, pp. 231–242.

[4] Price, S. J.,2001. "An Investigation on the use of Connors' Equation to predict Fluidelastic Instability in Cylinder Arrays". *Journal of Pressure Vessel Technology,* ***123***, pp. 448–453.

[5] Mahon, J., Meskell, C., 2012. "Surface pressure survey in a parallel triangular tube array. Journal or Fluids and Structures". *Journal or Fluids and Structures,* ***34***, pp. 123-137.

[6] Harran, G., 2014. "Influence of mass ratio on the fluidelastic instability of a flexible cylinder in a bundle of rigid tubes.". *Journal of Fluids and Structures,* ***47***, pp. 71–85.

[7] de Pedro, B. and Meskell, C., 2018. "Sensitivity of the damping controlled fluidelastic instability threshold to mass ratio, pitch ratio and Reynolds number in normal triangular arrays". *Nuclear Engineering and Design* ***331****, pp. 32–40*

[8] Meskell, C. and Fitzpatrick, J.A., 2003. "Investigation of the nonlinear behaviour of damping controlled fluidelastic instability in a normal triangular tube array". *Journal of Fluids and Structures* ***18****, pp. 573–593*

[9] de Pedro, B., Parrondo, J., Meskell, C., and Fernández-Oro, J.,2016. "CFD modelling of the cross-flow through normal triangular tube arrays with one tube undergoing forced vibrations or fluidelastic instability". *Journal of Fluids and Structures,* ***64***, pp. 67–86.

[10] Hassan, M., Gerber, A., and Omar, H., 2010. "Numerical Estimation of Fluidelastic Instability In Tube Arrays". *Journal of Pressure Vessel Technology, Transactions of the ASME,* ***132***, pp. 041307– (11 pp.).

[11] Parrondo, J., de Pedro, B., Fernández-Oro, J. and Blanco-Marigorta, E., 2017. "A CFD study on the fluctuating flow field across a parallel triangular array with one tube oscillating transversely". *Journal of Fluids and Structures,* ***76***, pp. 411–430.

[12] Mahon, J. and Meskell, C., 2009. "Surface pressure survey in normal triangular tube arrays. Journal or Fluids and Structures". *Journal or Fluids and Structures,* ***25***, pp. 1348-1368.

[13] Austermann, R. and Popp, K., 1999. "Stability Behaviour of a Single Flexible Cylinder in Rigid Tube Arrays of Different Geometry Subjected to Cross-Flow". *Journal of Fluids and Structures,* ***9***, pp. 303–322.

[14] Mahon, J. and Meskell, C., 2013. "Estimation of the time delay associated with damping controlled fluidelastic instability in a normal triangular tube array". *Journal of Fluids and Structures,* ***18***, pp. 573-593.

[15] Khalifa, A., Weaver, D. and Ziada, S., 2013. "An experimental study of flow-induced vibration and the associated flow perturbations in a parallel triangular tube array". *Journal of Pressure Vessel Technology,* ***135***, 030904 pp. 9.

[16] Sawadogo, T. and Murehithi, N., 2014. "Fluidelastic instability study in a rotated triangular tube array subject to two-phase cross-flow. Part I: Fluid force measurements and time delay extraction". *Journal of Fluids and Structures,* ***49 (1)***, pp. 1-15.

[17] Rzentkowski, G. and Lever, J.H., 1998. "An effect of turbulence on fluidelastic instability in tube bundles : a nonlinear analysis". *Journal of Fluids and Structures,* ***12 (5)***, pp. 561-590.